

Magnetotransport studies on the metallic side of the metal-insulator transition in PbTe

J. Oswald

Institut für Physik, Montanuniversität Leoben, A-8700 Leoben, Austria

B. B. Goldberg*

Department of Physics, Boston University, Boston, Massachusetts 02215

G. Bauer

Institut für Physik, Montanuniversität Leoben, A-8700 Leoben, Austria

P. J. Stiles

Department of Physics, Brown University, Providence, Rhode Island 02912

(Received 9 January 1989; revised manuscript received 17 April 1989)

The magnetotransport properties of n - and p -type PbTe with carrier concentrations ranging from 1.4×10^{16} to $1.05 \times 10^{17} \text{ cm}^{-3}$ were studied in fields up to 20 T and temperatures between 65 mK and 12 K. The data exhibit a strong temperature and magnetic field dependence in the extreme quantum limit. The longitudinal magnetoresistance of the sample with the smallest carrier concentration shows the most pronounced temperature dependence, similar in some respects to n -type $\text{Hg}_{1-x}\text{Cd}_x\text{Te}$ on the metallic side of the metal-insulator transition. In order to analyze the results, the Fermi energy is calculated as a function of magnetic field for the different magnetic field orientations investigated. It is shown that the range of experimental parameters accessed rules out a Wigner condensation according to the criteria given by Gerhardtts. Also, the region of a magnetic-field-induced Mott transition is just approached but not observed. In contrast to other narrow-band-gap semiconductors such as $\text{Hg}_{1-x}\text{Cd}_x\text{Te}$ and InSb, the static dielectric constant in PbTe is huge, and the free carriers originate definitively from vacancy states which form resonant levels deep within the bands. It is suggested that the observed magnetotransport phenomena are not the onset of a Mott-Anderson transition within an impurity band formed by donors, but rather due either (i) to fluctuating band edges, or (ii) a manifestation of a high-magnetic-field-induced Anderson transition driven by quantum-mechanical interferences due to scattering.

I. INTRODUCTION

The problem of low-temperature high-magnetic-field transport properties in $\text{Hg}_{1-x}\text{Cd}_x\text{Te}$ has caused a long-standing controversy.¹⁻³ The results have been interpreted either as evidence for magnetic freeze-out,^{4,5} as an Anderson-Mott transition,¹ or a Wigner condensation.^{2,3} Both n - and p -type PbTe, another narrow-band-gap material, were recently investigated,⁶ and the magnetotransport properties have exhibited a strong temperature dependence in the range 0.5–10 K, contrary to expectations. As pointed out by Nimtz *et al.*,⁷ PbTe seems to offer some interesting advantages for the observation and study of a Wigner condensate. In unintentionally doped samples, the free carriers originate from either Te or Pb vacancies which cause n - or p -type carrier conduction. The Te vacancy states form resonant levels within the conduction band,^{8,9} and magnetotransport measurements have not given any evidence for carrier freeze-out on localized states within the energy gap.¹⁰ In addition, due to a tendency towards a ferroelectric phase transition, the static dielectric constant in PbTe is very large and temperature dependent ($\epsilon_s > 1000$ at $T=4.2$ K). Therefore, the binding energy of hydrogenic donors is of the order of 1 μeV or less. At first glance, these conditions are not

favorable for a magnetic-field-induced Anderson-Mott transition. In addition, the huge dielectric constant does not favor Wigner condensation since the ratio of the potential energy ($\approx e^2/\epsilon_s r$) as compared to the kinetic energy ($\approx h^2/m^* r^2$) does not increase sufficiently strongly with increasing magnetic field. Nimtz *et al.*⁷ has found in PbTe and $\text{Pb}_{1-x}\text{Sn}_x\text{Te}$ a kink in $\rho_{xx}(B)$ as well as a decrease of the Hall coefficient, which is explained here as a transfer of carriers between Landau levels.

It is the purpose of this paper to present a systematic study of the transport properties of PbTe thin films in the temperature range between 65 mK and 12 K in magnetic fields up to 20 T. We investigate n -type and p -type samples in the extreme quantum limit, i.e., at sufficiently high magnetic fields that all carriers are in the lowest spin-split Landau state. In Sec. II we present the experimental results, and in Sec. III we compare the data with several models. The components of the magnetotransport tensor exhibit a substantial temperature dependence for magnetic fields which are too low to induce a Mott-Anderson-like transition for the given carrier concentrations, even if the existence of hydrogenic impurities is postulated. Also, the carrier concentrations are much too high for a Wigner condensation to be observable according to the criteria of Gerhardtts.¹¹ Finally, we summarize our conclusions in Sec. IV.

TABLE I. Sample parameters at $T=4.2$ K.

Sample	Carrier concentration (cm^{-3})	μ (cm^2/Vs)
<i>n</i> -type PbTe <i>A</i>	$n=1.4 \times 10^{16}$	550 000
<i>p</i> -type PbTe <i>B</i>	$p=6.4 \times 10^{16}$	19 000
<i>n</i> -type PbTe <i>C</i>	$n=1.1 \times 10^{17}$	

II. EXPERIMENTAL RESULTS

The PbTe samples are epitaxially grown films on [111]-oriented BaF_2 substrates deposited by a hot-wall technique.¹² The sample parameters are given in Table I. The measurements were performed in a ^3He - ^4He dilution refrigerator with fields produced by a Bitter magnet. Magnetoresistance and Hall effect were measured using a conventional ac lock-in technique ($f \approx 14\text{--}23$ Hz) with sample currents of the order of $5 \mu\text{A}$ (current density $j=0.6$ A/cm²). A Hall-bar geometry was defined photolithographically on the epitaxial film with current flow directed along the $[\bar{1}10]$. Therefore, the Hall resistance was measured with the magnetic field \mathbf{B} along [111] or $[11\bar{2}]$, and the longitudinal magnetoresistance ρ_{zz} with \mathbf{B} along the $[\bar{1}10]$.

In Fig. 1 the dependence of the transverse magnetoresistance $\rho_{xx}(B)$ on magnetic field as a function of temperature is shown for $\mathbf{B}||[111]$ and $\mathbf{B}||[11\bar{2}]$. Also shown is the Hall resistivity ρ_{xy} .

PbTe is a many-valley semiconductor with four equivalent extrema at the *L* point, both for the conduction and valence bands. The PbTe epitaxial film is elastically strained at low temperatures due to the difference in thermal contraction between the PbTe and BaF_2 . The elastic strain lifts the fourfold degeneracy of the *L* states for the growth direction ($||[111]$). The valley with its main axis parallel to [111] is shifted downwards in energy as compared to the three obliquely oriented valleys, for both the conduction and valence bands. The shift depends both on strain and on the components of the deformation-potential tensor and is of the order of 5 meV for PbTe on BaF_2 at $T \approx 4.2$ K.¹³

In order to correlate structures in the magnetoresistance with the population of the Landau level, it is necessary to calculate the magnetic field dependence of the Fermi level. For the numerical calculation of the Landau levels a (4×4) $\mathbf{k} \cdot \mathbf{p}$ band model was used,¹⁴ taking into account the strain-induced energy shift between the obliquely oriented valleys and that oriented parallel to the [111]. Band parameters are given in Ref. 15. The Landau levels and resulting variation of the Fermi energy versus B are shown in the insets to Fig. 1. The calculation shows that the [111] valley becomes depopulated at a field of about 12 T for $\mathbf{B}||[111]$ due to carrier transfer into the lowest Landau states of the three oblique valleys [Figs. 1(a) and 1(c) insets]. For $\mathbf{B}||[11\bar{2}]$ three different Landau ladders are involved. However, just one valley is populated for $\theta=90^\circ$ (θ is the angle between \mathbf{B} and the main-valley axis). The apparent kink in $\rho_{xx}(B)$ at $B \approx 3$ T for $\mathbf{B}||[11\bar{2}]$ is caused by the movement of the Fermi level from the 0^+ to the 0^- state within one Landau level as

shown in the inset to Fig. 1(b). Since the decrease of the kinetic energy of the carriers with increasing magnetic field is important for further comparisons of experimental results with theoretical models, we also plot the variation of the Fermi energy with respect to the lowest occupied Landau states (either 0^- in [111] or 0^- in $[\bar{1}\bar{1}1]$) in the inset to Fig. 1(c). For $\mathbf{B}||[111]$ the kinetic energy becomes as small as 10^{-2} meV at the highest field in a $T=0$ approximation for the lowest-concentration sample *A*.

In Fig. 2 the longitudinal magnetoresistance ρ_{zz} of sample *A* is plotted versus B for $\mathbf{B}||[\bar{1}10]$. A nearly linear dependence of the longitudinal magnetoresistance

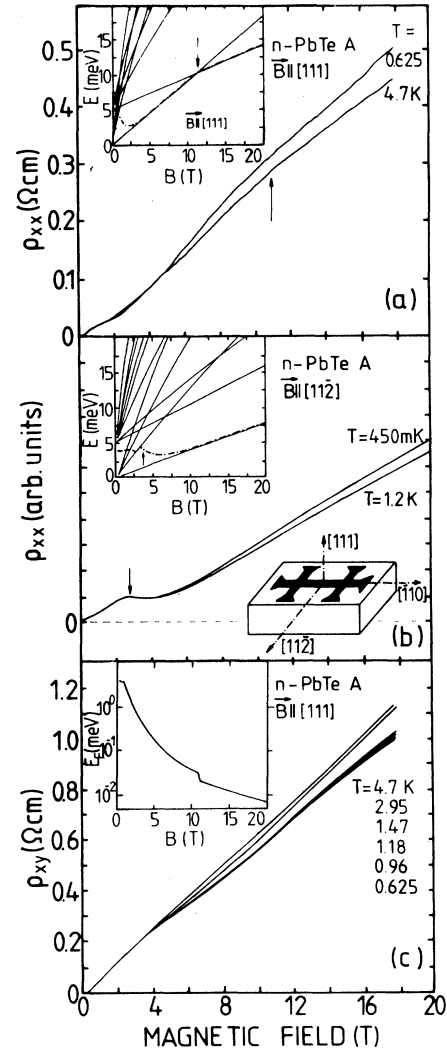


FIG. 1. (a) Transverse magnetoresistance ρ_{xx} vs B for $\mathbf{B}||[111]$ for sample *A*. Arrow indicates carrier transfer from the lowest 0^- states of [111] valley to the lowest 0^- states of the oblique valleys. Inset: Landau states for $\mathbf{B}||[111]$, oblique valleys shifted by $\Delta=5$ meV upwards. The dashed-dotted line is the Fermi energy E_F . (b) ρ_{xx} vs B for $\mathbf{B}||[11\bar{2}]$; all other parameters as for (a). Lower inset shows the sample Hall-bar geometry and orientations. (c) Hall resistance ρ_{xy} vs B for $\mathbf{B}||[111]$ for sample *A*. Inset indicates variation of Fermi energy with respect to the lowest 0^- state.

on the magnetic field over a wide range was found earlier by Allgaier.¹⁶ In this configuration the temperature dependence is much more pronounced in the high fields. To demonstrate the onset of this behavior, the lower half of Fig. 2 shows a restricted low-magnetic-field region. In this configuration, two valleys are oriented with respect to \mathbf{B} by $\theta=90^\circ$. Due to the built-in strain, just one valley is populated for $B \geq 3$ T when the Fermi level drops into the 0^- Landau state. Because a single level is occupied, the Fermi energy approaches a value of only 10^{-1} meV with respect to the 0^- state (versus 10^{-2} meV for the case of ρ_{xx} and ρ_{xy} when three levels are occupied for $\mathbf{B}||[111]$).

In Fig. 3 we show similar data and calculations of the Landau levels for a p -type sample (B) which has a

significantly greater carrier concentration. Due to strain, the three obliquely oriented valleys are populated for all concentrations at $B=0$. For sufficiently high hole concentrations, the valley with its main axis parallel to $[111]$ also becomes populated at $B=0$. Even for the comparatively high carrier concentration of sample B , the Fermi level approaches the lowest 0^- Landau state with an energy of the order of 10^{-1} meV at the highest magnetic fields.

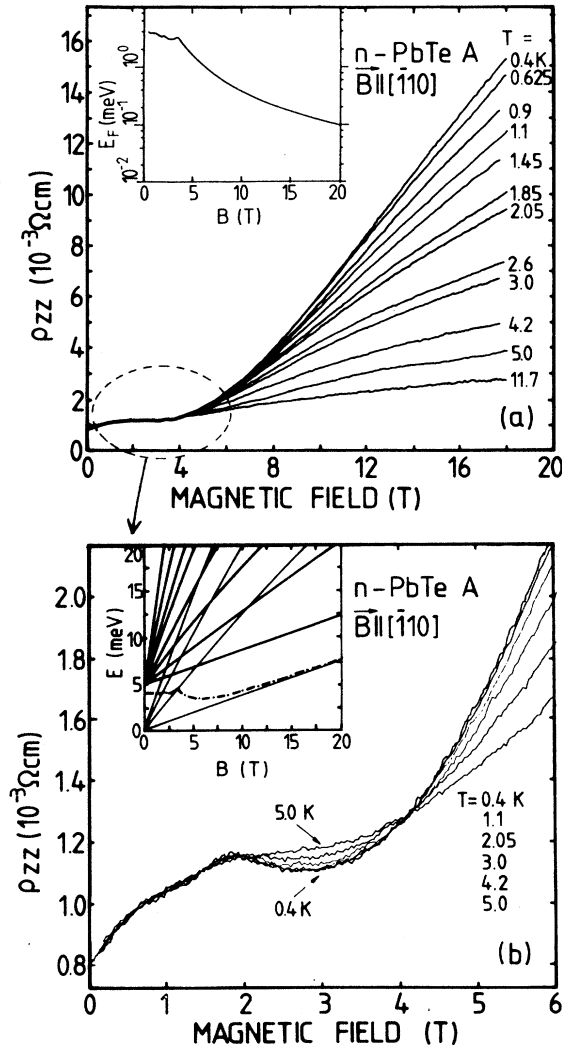


FIG. 2. (a) Longitudinal magnetoresistance vs B for $\mathbf{B}||[110]$. Inset: Fermi level with respect to the lowest Landau state 0^- (of the valley oriented with $\theta=90^\circ$ with respect to \mathbf{B}). (b) Low-magnetic-field portion of (a). Inset: Landau states for $\mathbf{B}||[110]$; $\theta=35^\circ$, 26° , and 90° . One of the $\theta=90^\circ$ valleys and the two $\theta=35^\circ$, 26° valleys are shifted upwards by 5 meV.

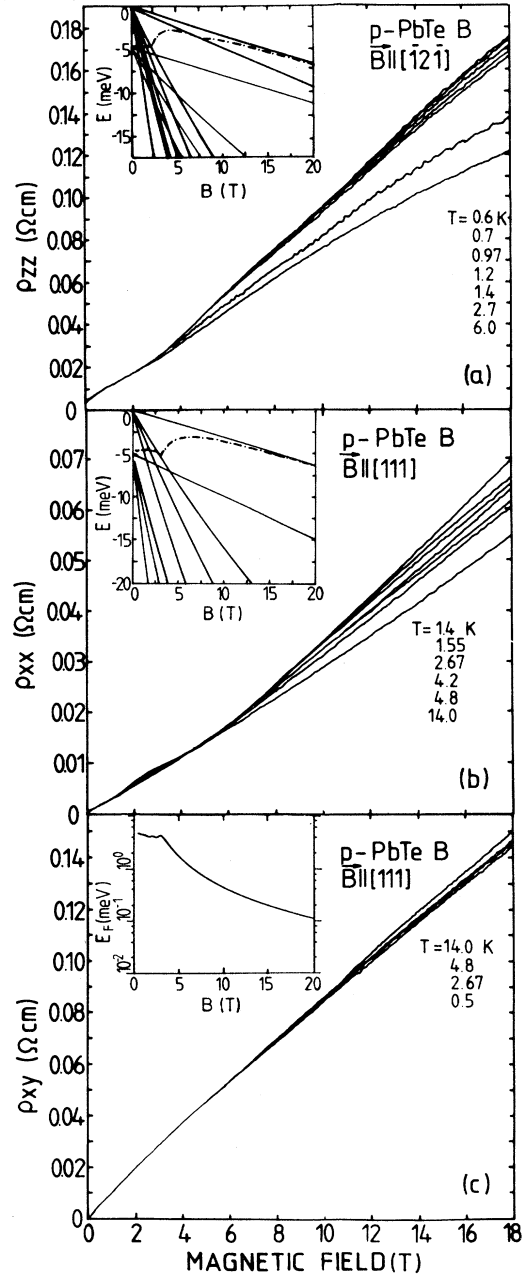


FIG. 3. (a) ρ_{zz} vs B for the p -type sample B . Inset shows the Landau states and $E_F(B)$. (b) Transverse magnetoresistance ρ_{xx} vs B for $\mathbf{B}||[111]$. Inset: Landau states and $E_F(B)$. (c) Hall resistance ρ_{xy} vs B . Inset: Fermi level with respect to the lowest occupied 0^- states of the three oblique valleys.

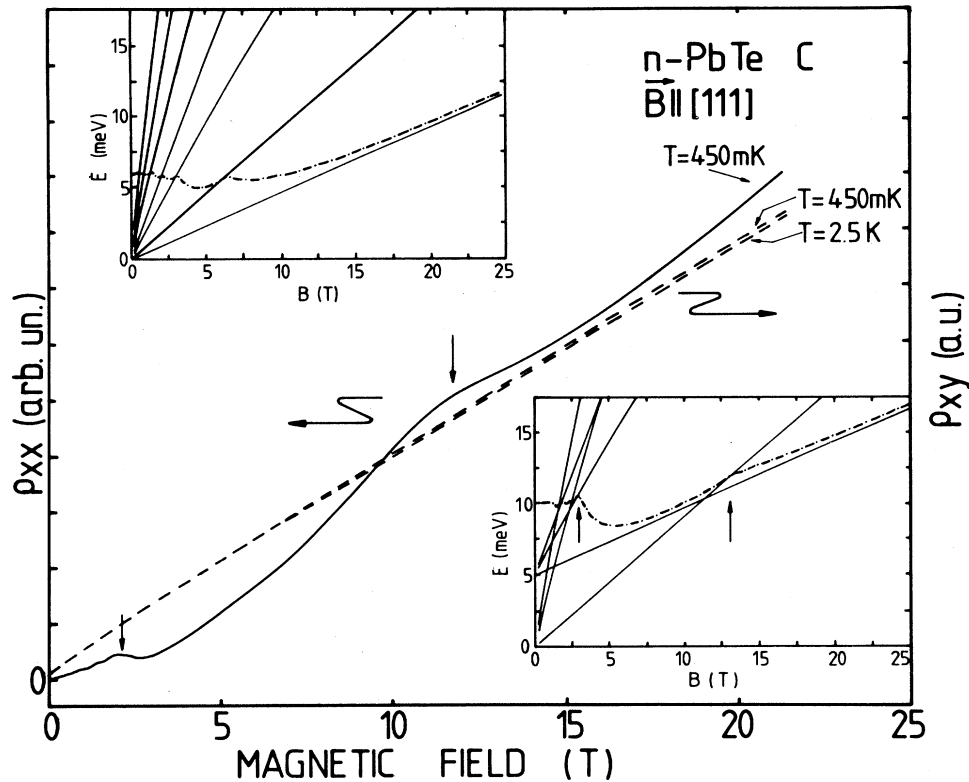


FIG. 4. ρ_{xx} and ρ_{xy} vs B for n -type sample C ($n = 1.05 \times 10^{17} \text{ cm}^{-3}$). Lower inset: Landau states of the $\theta = 0^\circ$ and the three $\theta = 70.53^\circ$ valleys vs B . The dashed-dotted line is the Fermi level, and the arrows indicate the transitions to the 0^- ($\theta = 0^\circ$) and 0^- ($\theta = 70.53^\circ$) states with increasing B . Upper inset is same as lower, but without the strain which shifts the $\theta = 70.53^\circ$ valleys included in the calculation ($\Delta = 0 \text{ meV}$).

In Fig. 4 ρ_{xx} and ρ_{xy} versus B are shown again for an n -type sample with the higher carrier concentration ($1.1 \times 10^{17} \text{ cm}^{-3}$). The temperature dependence is now very small, and the Fermi level remains well above 1 meV with respect to the lowest 0^- states of the oblique valley for $\mathbf{B} \parallel [111]$ even at $B = 20 \text{ T}$. The insets demonstrate the correctness of the strain energy of $\Delta = 5 \text{ meV}$ by the matching of the maxima of the experimentally observed Shubnikov–de Haas–like oscillations in ρ_{xx} to the calculation. The upper left inset is calculated with no strain energy ($\Delta = 0 \text{ meV}$), while the lower right inset is calculated with $\Delta = 5 \text{ meV}$. The arrows in the lower right inset indicate changes in the population of the levels that clearly correspond to the experimentally observed kinks. Features derived from the calculations and appearing in the magnetotransport are evident in all the samples (see Figs. 1–3) and lend confidence to the strain energy and calculated Landau states, as well as explaining previous data.⁷

All experimental data on the Hall effect show a decrease of ρ_{xy} with increasing magnetic field that becomes more pronounced for lower temperatures. In the sample with the lowest concentration (A), the effect is much larger than in B or C . It seems worthwhile to compare this behavior with $\text{Hg}_{1-x}\text{Cd}_x\text{Te}$,¹ where a similar dependence of $\rho_{xy}(B)$ is observed in an intermediate-field range. For sufficiently high fields, this so called ‘‘Hall dip’’

disappears in $\text{Hg}_{1-x}\text{Cd}_x\text{Te}$ since the freeze-out of carriers causes $R_H = \rho_{xy}/B$ to increase substantially above its zero-magnetic-field value. Such a behavior is not observed in either n - or p -type PbTe .

In Fig. 5 the Hall-coefficient ratio $R_H(B)/R_H(B \rightarrow 0)$ is shown for sample A versus magnetic field in the temperature range between 600 mK and 4.7 K.

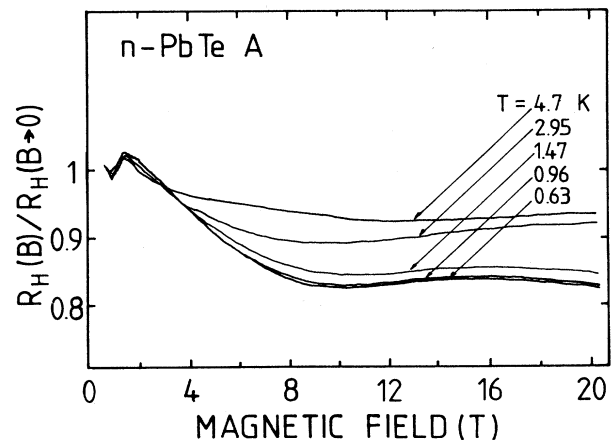


FIG. 5. Hall-coefficient ratio $R_H(B)/R_H(B \rightarrow 0)$ vs magnetic field B for sample A ($n = 1.4 \times 10^{16} \text{ cm}^{-3}$).

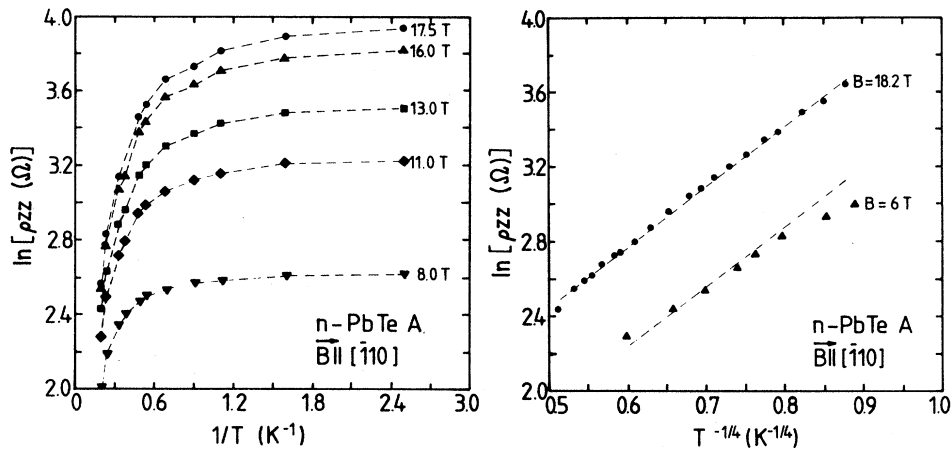


FIG. 6. (a) $\ln \rho_{zz}$ vs T^{-1} for sample *A* for a number of different magnetic fields. (b) $\ln \rho_{zz}$ vs $T^{-1/4}$ for sample *A* for two magnetic fields.

III. DISCUSSION

It is evident from the data shown in the preceding section, especially the Hall data of Fig. 5, that no indication for an activated behavior of the carrier concentration can be found in *n*- or *p*-type PbTe in the investigated temperature and magnetic field range, in direct contrast to $\text{Hg}_{1-x}\text{Cd}_x\text{Te}$ (Ref. 1) and InSb.¹ Since the longitudinal magnetoresistance ρ_{zz} exhibits the most dramatic temperature dependence in PbTe, $\ln \rho_{zz}$ of sample *A* is plotted versus T^{-1} in Fig. 6(a) and versus $T^{-1/4}$ in Fig. 6(b) for a few magnetic field values. In the temperature range of interest, no clear dependence $\ln \rho_{zz} \sim T^{-1}$ is observed up to 17.5 T. A $T^{-1/4}$ dependence exists weakly for $T > 1$ K, but fails at lower temperatures where ρ_{zz} saturates [outside the range of Fig. 6(b), but apparent in Fig. 6(a)].

In other narrow-band-gap materials ($\text{Hg}_{1-x}\text{Cd}_x\text{Te}$ and *n*-type InSb) the onset of a metal-insulator transition was deduced from the application of a theory by Lee and Ramakrishnan¹⁷ for the longitudinal magnetoresistance in disordered metals in weak magnetic fields. According to Ref. 17, $\sigma_{zz} = \rho_{zz}^{-1}$ should vary with temperature according to

$$\sigma_{zz} = \sigma_0 + aT^{1/2} + bT, \quad (1)$$

where the $aT^{1/2}$ term is due to Coulomb interactions and the bT term is due to localization effects. In Fig. 7 plots of σ_{zz} versus $T^{1/2}$ for a succession of magnetic fields are shown with parameter fits according to Eq. (1). Though the general shape of $\sigma_{zz}(B)$ looks similar to those found in $\text{Hg}_{1-x}\text{Cd}_x\text{Te}$ (Ref. 1) and InSb,^{1,18} there remains a systematic difference: zero longitudinal conductivity as $T \rightarrow 0$ is not approached even for the highest fields. Since a minimum metallic conductivity exists, no magnetic-field-induced metal-insulator transition can be inferred from the data. The parameter fits yield a value of 0.5 for a for all the magnetic fields, while b ranges from 40 to 46, indicating that the linear term dominates the temperature dependence.

The fits to Eq. (1) show that there is a large deviation at low temperatures where σ_{zz} exhibits a loss of tempera-

ture dependence. This is in marked contrast to *n*-type InSb, where Mansfield *et al.*¹⁸ have found that Eq. (1) produces an excellent fit for samples with $n = 6.7 \times 10^{15} \text{ cm}^{-3}$ in the temperature range 30 mK–1 K.

In Fig. 8 we plot results of the low-temperature longitudinal magnetoresistance in sample *A*. ρ_{zz} versus B for temperatures between 65 mK and 1.18 K is shown with the T dependence at 19.7 T exhibited in the inset. The increase in ρ_{zz} for decreasing temperature disappears below $T \approx 350$ mK, saturating completely. It is highly unlikely that this saturation is due to a metallic parallel conducting channel, as is the case in $\text{Hg}_{1-x}\text{Cd}_x\text{Te}$.¹ First, a metallic surface (or otherwise parallel conducting) layer would be expected to cause a convergence of the high-field, low-temperature magnetotransport curves since the resistance of the parallel channel would be relatively temperature and magnetic field independent, and would dominate the transport whenever the magnetoresistance of the sample became greater. The data on PbTe show no such convergence, and, in fact, show vanishing tempera-

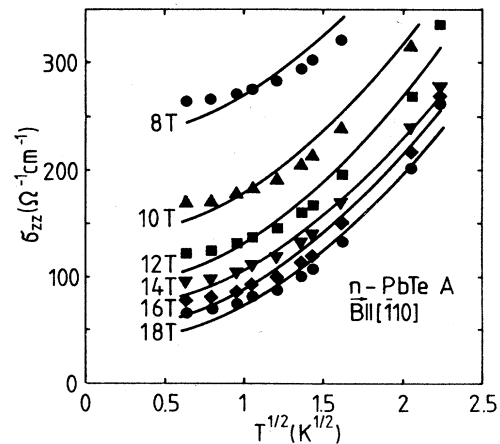


FIG. 7. σ_{zz} vs \sqrt{T} for sample *A* magnetic fields from 8 to 18 T. Solid lines are fit to the data (see text).

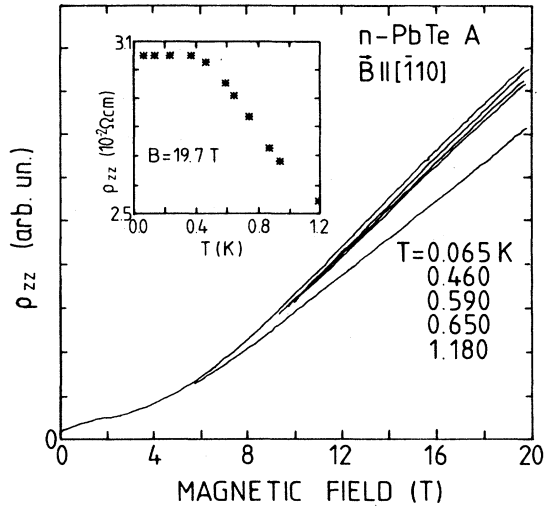


FIG. 8. Low-temperature magnetoresistance of sample A. $\rho_{zz}(B)$ saturates for $T \leq 350$ mK. Inset shows the temperature dependence of ρ_{zz} from 65 mK to 1.18 K at $B = 19$ T.

ture dependence at the same temperature at any magnetic field above ~ 5 T, over a wide range in the magnitude of the resistance of the sample. The anomalous temperature-dependent increase in ρ_{zz} and the final saturation must be due to the same physical mechanism since they are observed over the same parameter range. Second, ρ_{xx} saturates at the same temperature but at a much greater (factor of 20) resistance. And third, the kinks occurring in ρ_{xx} at 13 T and 0.6 K are well described by the inclusion of strain in the band structure and the transfer of carriers between Landau levels, indicating that the transport is not dominated by a parallel conducting channel, though the sample is well into the regime where the saturation and unusual temperature-dependent effects are observed.

In Fig. 9 the experimental data of σ_{zz} are plotted versus $B^{-2.2}$ in order to get an estimate of the magnetic

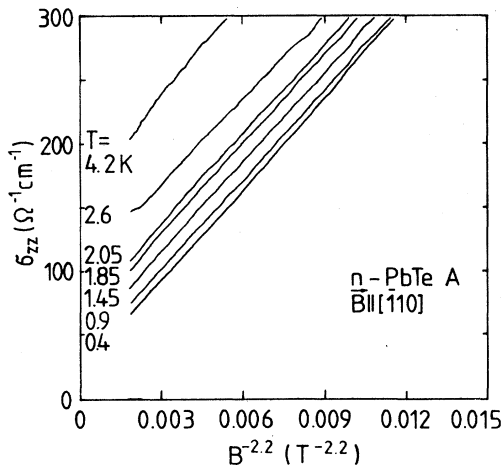


FIG. 9. σ_{zz} vs $B^{-2.2}$ for a range of temperatures from 0.4 to 4.2 K. Note that magnetic fields in excess of 50 T would be necessary to observe a vanishing conductivity.

field required to observe a vanishing longitudinal conductivity. The exponent $m = 2.2$ was simply adjusted to yield a straight-line fit for $\sigma_{zz} \propto B^m$. From the figure it is evident that magnetic fields in excess of 50 T would be necessary to induce a metal-insulator transition.

In InSb and $\text{Hg}_{1-x}\text{Cd}_x\text{Te}$ the critical field for the magnetic-field-induced metal-insulator transition has been estimated with the aid of a Mott criterion,¹⁹

$$n(a_{\perp}^*)^2(a_{\parallel}^*) = \delta^3, \quad (2)$$

where $a_{\perp}^* = 2l = 2(\hbar/eB)^{1/2}$ and $a_{\parallel}^* = a^*/\ln\gamma$, $\gamma = \hbar\omega_c / 2R = (a^*/l)^2$, and δ is a constant, approximately 0.3. R is the effective Rydberg energy of hydrogenic donors, and a^* is the Bohr radius. Due to the large dielectric constant, the effective Bohr radius is huge, about 10^4 Å. The critical concentration of donors, N_D , in a magnetic field of 10 T is $N_D = 1 \times 10^{15} \text{ cm}^{-3}$ (same as the carrier concentration n for uncompensated samples), which is a comparatively small value for a typical PbTe sample. For the carrier concentration of sample A ($n = 1.4 \times 10^{16} \text{ cm}^{-3}$), Eq. (2) yields a critical magnetic field of 105 T—a factor of 5 higher than the largest field experimentally investigated.

The redistribution of carriers between band and impurity states with decreasing temperature and increasing field was demonstrated conclusively by far-infrared magneto-optical experiments in $\text{Hg}_{1-x}\text{Cd}_x\text{Te}$ by Shayegan *et al.*¹ No definite evidence for an impurity band can be deduced from our magnetotransport data, despite the depression of R_H (Fig. 5). Explanations for the “Hall dip” include conduction through an infinite metallic cluster separated by nonconducting regions,¹ and two-band transport where hybrid impurity and band states with different densities and mobilities account for $R_H(B)$ in $\text{Hg}_{1-x}\text{Cd}_x\text{Te}$. These models all depend on the eventual upturn in $R_H(B)$, caused by the “freeze-out” of carriers. Figure 5 implies some dependence of $R_H(B)$ without the rapid increase beyond a critical field due to a Mott transition. Since this increase in $R_H(B)$ is not observed, the critical temperature and magnetic field estimates are nearly an order of magnitude off, and the data show a nonvanishing conductivity as $T \rightarrow 0$; a metal-insulator transition occurring in an impurity band cannot be postulated to account for the temperature-dependent magnetotransport in PbTe.

The possibility of Wigner crystallization induced by a magnetic field has been suggested by Nimtz and Schlicht⁷ as an explanation for the kinks in the magnetotransport of PbTe, and has received much attention for the other narrow-gap semiconductors. Gerhardts¹¹ has estimated the critical temperature and magnetic field and used these estimates to generate a type of phase diagram. Some controversy exists over the use of a Hartree-Fock approximation for a system of interacting electrons,¹¹ and the effect this has on the dependence of the melting temperature in the high-field limit.² For our purposes, the expressions of Ref. 11 give adequate estimates for the critical temperature and field of the Wigner transition in PbTe.

Wigner condensation of the electrons occurs when the critical value of the ratio of the potential energy and the

mean kinetic energy $\Gamma = \langle V \rangle / E_{\text{kin}}$ reaches¹¹ $\Gamma \sim 8$. Using PbTe parameters for the mean distance between electrons, $r = (4\pi n/3)^{-1/3}$, and for $a^* = a_B \epsilon_n m_0 / m^*$, we obtain a critical carrier concentration for which $r > 7a^*$; $n_{\text{crit}} = 1 \times 10^{11} \text{ cm}^{-3}$. Condensation in PbTe is therefore impossible to observe without a magnetic field.

In the presence of a magnetic field, the mean carrier energy decreases like the Fermi energy (see Figs. 1–3). The potential energy is fixed by the interelectron distance r_s , which is given by the carrier concentration (for sample A, $\langle V \rangle \approx 55 \text{ } \mu\text{eV}$). Hence Γ increases with B as $[E_F(B)]^{-1}$. Also the sample temperature must be less than the Fermi temperature T_F . Thus, applying the criterion $r_s > 7a^*$ yields both a temperature below 70 mK and a magnetic field in excess of 70 T for $\mathbf{B} \parallel [110]$. We note that since E_F depends strongly on the magnitude and orientation of the magnetic field for the thin-film PbTe samples, the critical values will as well.

Order-of-magnitude estimation based on the phase diagram of Gerhardtts¹¹ yields critical temperatures comparable to the Rydberg temperature, $T_c \approx 20 \text{ mK}$. Magnetic fields higher than 20 T would not help to change this situation since the melting temperature of the Wigner condensate saturates for sufficiently high fields.² The experimental temperatures in this study are a factor of 3 too high for the Gerhardtts criteria to be fulfilled, yet the complete saturation of the magnetoresistance at low temperatures supports the conclusion that no Wigner transition is occurring. Finally, it is difficult to obtain clear evidence for Wigner condensation from transport experiments, even in the “viscous state.”^{2,7,20}

All estimates on Wigner condensation assume the jellium model. This is better fulfilled in the situation of PbTe than in the other narrow-band-gap semiconductors, since the carriers in PbTe originate from vacancies and ϵ_s is extremely large. Nevertheless, the vacancy states produce randomly distributed charges which cause fluctuations of the band edge.¹⁹ In order to estimate these fluctuations and their effect, a value of the compensation ratio $K = \|V_{\text{Te}}\| / \|V_{\text{Pb}}\|$ is required. From the mobility data of sample A and the results of Ref. 21, we get, $K = 0.7$. The average electric field due to vacancies is then given by¹⁹

$$\begin{aligned} \bar{E}_m &= 6eN_{\parallel\text{Te}}^{2/3} \frac{1}{4\pi\epsilon_s\epsilon_0} \\ &= 1.9 \times 10^4 \text{ V/m} . \end{aligned} \quad (3)$$

Thus the band-edge fluctuations are 0.56 meV for doubly charged vacancies spaced by the corresponding mean distance. The Fermi energy E_F is above this fluctuating potential in all samples at $B = 0$. For sufficiently high fields, E_F becomes comparable and even smaller than the band-edge fluctuations. However, at fields where E_F is less than the fluctuations ($E_F < 10^{-1} \text{ meV}$ at $B = 12 \text{ T}$ in sample A), the carriers continue to behave according to the band effective mass as evidenced by the coincidence of the kink in ρ_{xx} and calculated E_F dependence. The metal-insulator transition causes changes in the effective mass in InSb,²² and a redistribution of carriers between

band and impurity states in $\text{Hg}_{1-x}\text{Cd}_x\text{Te}$ (Ref. 1) that is not observed in the PbTe data.

The low-temperature transport of sufficiently pure PbTe is governed by carrier scattering due to the short-range potential of the intrinsic vacancies. This is quite different from the ordinary Coulomb scattering by charged impurities in InSb and $\text{Hg}_{1-x}\text{Cd}_x\text{Te}$. Anderson localization occurs in systems in which the inverse Fermi wave vector k_F^{-1} becomes comparable to the scattering length l_e due to quantum-interference effects. However, it has been established that weak magnetic fields destroy this type of Anderson localization by breaking the symmetry with respect to forward- and backward-scattering events.^{23,24} If the magnetic field is so strong that only the lowest Landau subband is occupied, the electronic motion becomes quasi-one-dimensional along the field direction. For high enough fields the Fermi wavelength becomes comparable to the carrier mean free path (extended in PbTe due to the dominant scattering mechanism) and Anderson localization may occur. Recently, Ono and Ohtsuki²⁵ have applied a self-consistent theory of Anderson localization to three-dimensional systems under quantizing magnetic fields and derived the critical behavior of the diagonal conductivities. They estimate the critical magnetic field as

$$(E_F / \hbar\tau)^{1/4} (E_F / \hbar\omega_c) = 0.509 , \quad (4)$$

where E_F denotes the zero-field Fermi energy, τ the scattering time, and $\hbar\omega_c$ the Landau-level separation. Using the parameters of sample A, values for the left-hand side of Eq. (4) in the range 0.5–1.1 are obtained, depending on the orientation of the magnetic field. This model leads to an explanation of the onset of a metal-insulator transition in PbTe driven by Anderson localization induced by quantum-mechanical interference effects. This is especially appealing since the vacancies are resonant, well above the conduction band in n -type PbTe. Even if hydrogenic or other impurities were present in PbTe, their number would be few and not directly related to the number of vacancies. The vacancy potential is δ -like, but it is difficult to imagine that actual bound states can be induced. Drew²⁶ has suggested that central-cell effects might lead to binding energies of 2–3 meV in high magnetic fields, but this model requires impurity states as well. The high-field scattering model for the Anderson localization avoids these difficulties.

Finally, we argue that the observed temperature dependencies of ρ_{zz} and ρ_{xx} are not a consequence of a transition from a degenerate electron gas to one which obeys classical statistics. Though E_F becomes small and comparable to $k_B T$ in high magnetic fields, T -dependent effects on the magnetotransport are apparent at temperatures above 1 K, when $T_F > T$. It is also unlikely that the interface region between the BaF_2 substrate and PbTe high-quality film is causing the observed unusual temperature dependence in the magnetotransport. First, the interface region is of much lower mobility and thickness than the films, and, second, the interface is heavily p type and the temperature dependence is seen in both n - and p -type films.

IV. CONCLUSIONS

The magnetotransport coefficients of PbTe with carrier concentrations of the order of 10^{16} – 10^{17} cm⁻³ exhibit some interesting similarities to those reported for *n*-type Hg_{1-x}Cd_xTe. The longitudinal magnetoresistance has a substantial temperature dependence between $T=0.4$ and 10 K. Since the free carriers in *n*-type PbTe originate from vacancies which form resonant levels deep in the conduction band, a magnetic-field-driven metal-insulator transition in an impurity band is not plausible. If the presence of hydrogenic impurities is assumed, applying the Mott criterion means the sample concentrations are at least a factor of 10 too high for establishing the metal-insulator transition. Wigner condensation is ruled out both by the low-temperature saturation of the longitudinal conductivity, and by the fact that the range of temperatures and magnetic fields investigated is well outside the Gerhardt's¹¹ criteria.

The statistical distribution of vacancy states causes a fluctuating potential superimposed on the band edges of the order of 0.5 meV. These band-edge fluctuations could provide a basis for the observed dependencies of ρ_{xx} , ρ_{zz} , and ρ_{xy} on T and B . Additionally, the increase in ρ_{zz} for decreasing temperature and increasing field could be the

onset of an Anderson transition driven by quantum-mechanical interference effects in the extreme magnetic quantum limit. Applying a criterion by Ono²⁴ shows this is possible, even in the case where E_F is larger than the band-edge fluctuations.

In order to get further information necessary for the application of the ideas on Anderson localization and band-edge-fluctuation effects, additional magnetotransport and magneto-optical experiments are planned.

ACKNOWLEDGMENTS

This work was supported by Fonds zur Förderung der wissenschaftlichen Forschung (Vienna), under Project No. P5841, and by the U.S. National Science Foundation under Grant No. DMR-87-17817 and No. DMR-85-11789. One of us (B.B.G.) acknowledges partial support by the Massachusetts Institute of Technology, and thanks J. E. Furneaux for valuable discussions. G. B. and J. O. thank T. Dietl for many helpful discussions. We thank B. Brandt and L. Rubin of the Francis Bitter National Magnet Laboratory for technical assistance, and A. Lopez-Otero and L. D. Haas for the growth of the samples.

*Also at Francis Bitter National Magnet Laboratory, Massachusetts Institute of Technology, Cambridge, MA 02139.

¹M. Shayegan, V. J. Goldman, and H. D. Drew, Phys. Rev. B **38**, 5585 (1988), and references cited therein.

²S. B. Field, D. H. Reich, T. F. Rosenbaum, P. B. Littlewood, and D. A. Nelson, Phys. Rev. B **38**, 1856 (1988).

³G. Nimitz and J. Gebhardt, in *Proceedings of the 18th International Conference on the Physics of Semiconductors*, edited by O. Engström (World Scientific, Singapore, 1987), p. 1197.

⁴A. Raymond, J. L. Robert, R. L. Aulombard, C. Bousquet, O. Valassiades, and M. Royer, in *Physics of Narrow Gap Semiconductors*, Vol. 152 of *Springer Lecture Notes in Physics*, edited by E. Gornick, H. Heinrich, and L. Palmethofer (Springer, Berlin, 1982), p. 387.

⁵F. Herlach and G. de Vos, J. Phys. C **20**, 5901 (1987).

⁶J. Oswald, B. B. Goldberg, G. Bauer, and P. J. Stiles, in *Proceedings of the International Conference on Applications in High Magnetic Fields in Semiconductor Physics*, Würzburg (1988) *Springer Series in Solid State Sciences*, edited by G. Landwehr.

⁷G. Nimitz and B. Schlicht, in *Festkörperprobleme (Advances in Solid State Physics)*, edited by P. Grosse (Vieweg, Braunschweig, 1980), Vol. XX, p. 369.

⁸B. A. Volkov and O. A. Pankratov, Zh. Eksp. Teor. Fiz. **88**, 280 (1985) [Sov. Phys.—JETP **61**, 164 (1985)]; K. Lischka, Phys. Status Solidi B **133**, 17 (1986); O. A. Pankratov and P. P. Povarov, Solid State Commun. **66**, 847 (1988).

⁹N. G. Parada and G. W. Pratt, Phys. Rev. Lett. **22**, 183 (1969); N. G. Parada, Phys. Rev. B **3**, 2042 (1970).

¹⁰G. Bauer, H. Burkhard, H. Heinrich, and A. Lopez-Otero, J.

Appl. Phys. **47**, 1721 (1976).

¹¹R. R. Gerhardt, in *High Magnetic Fields in Semiconductor Physics: Proceedings of the International Conference, Würzburg, 1986*, Vol. 71 of *Springer Series in Solid State Sciences*, edited by G. Landwehr (Springer, Berlin, 1987), p. 482.

¹²A. Lopez-Otero, Thin Solid Films **49**, 3 (1978).

¹³J. Singleton, E. Kress-Rogers, A. V. Lewis, R. J. Nicholas, E. J. Fantner, G. Bauer, and A. Lopez-Otero, J. Phys. C **19**, 77 (1986).

¹⁴H. Burkhard, G. Bauer, and W. Zawadzki, Phys. Rev. B **19**, 5149 (1979).

¹⁵H. Pascher and G. Bauer, in Ref. 11, p. 400.

¹⁶R. S. Allgaier, J. Appl. Phys. **59**, 1388 (1986).

¹⁷P. A. Lee and T. V. Ramakrishnan, Rev. Mod. Phys. **57**, 287 (1985).

¹⁸R. Mansfield, M. Abdul-Gader, and P. Fozooni, Solid State Electron. **28**, 109 (1985).

¹⁹B. I. Shklovskii and A. L. Efros, *Electronic Properties of Doped Semiconductors* (Springer-Verlag, New York, 1984).

²⁰I. M. Tsidilkovskii, Usp. Fiz. Nauk **152**, 583 (1987) [Sov. Phys.—Usp. **30**, 676 (1987)].

²¹L. Palmethofer, K. H. Gresslehner, L. Ratschbacher, and A. Lopez-Otero, in Ref. 4, p. 468.

²²S. Ishida and E. Otsuka, J. Phys. Soc. Jpn. **43**, 124 (1977).

²³For example, S. Hikami, A. I. Larkin, and Y. Nagaoka, Prog. Theor. Phys. **63**, 707 (1980).

²⁴T. Ohtsuki, and Y. Ono, J. Phys. Soc. Jpn. **55**, 2347 (1986).

²⁵Y. Ono, and T. Ohtsuki, in Ref. 11, p. 377.

²⁶H. D. Drew (unpublished).